

Light-particle correlations with evaporation residues in the $^{40}\text{Ca}+^{12}\text{C}$ reaction at $E(^{40}\text{Ca})=450$ MeV

M. F. Vineyard,¹ S. E. Atencio,¹ J. F. Crum,¹ G. P. Gilfoyle,¹ B. G. Glagola,² D. J. Henderson,²
D. G. Kovar,^{2,*} C. F. Maguire,³ J. F. Mateja,⁴ R. G. Ohl,¹ F. W. Prosser,⁵ J. H. Rollinson,¹ and R. S. Trotter¹

¹*Department of Physics, University of Richmond, Richmond, Virginia 23173*

²*Physics Division, Argonne National Laboratory, Argonne, Illinois 60439*

³*Department of Physics and Astronomy, Vanderbilt University, Nashville, Tennessee 37235*

⁴*Division of Educational Programs, Argonne National Laboratory, Argonne, Illinois 60439*

⁵*Department of Physics, University of Kansas, Lawrence, Kansas 66045*

(Received 7 September 1993)

Proton and α -particle correlations with evaporation residues were measured over the complete angular range in the interaction of a 450-MeV ^{40}Ca beam with a ^{12}C target. Comparisons of the data with predictions of the statistical model and expectations for complete fusion from the kinematics provide clear and consistent evidence of incomplete fusion due to pre-equilibrium emission of both protons and α particles from the ^{12}C target. However, there is conflicting evidence both for and against preequilibrium emission from the projectile.

PACS number(s): 25.70.Jj, 25.70.Mn

I. INTRODUCTION

The study of linear-momentum transfer in relatively light, heavy-ion systems ($A_{\text{projectile}} + A_{\text{target}} \leq 60$) at bombarding energies around and above 10 MeV/nucleon has received considerable attention in recent years [1–10]. In these studies, the velocity distributions of evaporation residues are compared to that expected for a complete-fusion reaction in which the full linear momentum of the projectile is transferred to the compound nucleus. In studies of reactions involving asymmetric systems in which the projectile is lighter than the target, the velocity centroids of the heavy residues are found to be shifted to lower velocities than expected for full linear-momentum transfer. When the projectile is heavier than the target, the distributions are shifted to higher velocities than expected. For symmetric systems, a broadening of the velocity distributions rather than a shift in the centroids is observed. These results have been interpreted as evidence that some fraction of the evaporation residues arise from a composite nucleus, formed in a preequilibrium or incomplete-fusion process, that is moving at a different velocity than the complete-fusion compound nucleus due to the emission of preequilibrium particles. This behavior is qualitatively consistent with the picture that particle emission from (or breakup of) the projectile and/or target occurs (some fraction of the time) prior to fusion, and that the emission from the lighter reaction partner is dominant.

The origin of the preequilibrium emission of light particles associated with incomplete fusion is unknown and

one of the interesting questions is whether the incomplete momentum transfer is the result of the emission of predominantly nucleons or of heavier particles. Several coincidence experiments [11–15] have been performed to investigate preequilibrium emission in these relatively light systems. The results of three studies of rather asymmetric systems [11–13] indicate that preequilibrium α emission plays an important role. In a study of the $^{20}\text{Ne}+^{27}\text{Al}$ reaction at $E(^{20}\text{Ne})=19.2$ MeV/nucleon, a preequilibrium α component was identified; however, it was determined that it accounted for at most $\frac{1}{3}$ of the momentum lost in the incomplete fusion process [14]. On the other hand, measurements for the $^{14}\text{N}+^{12}\text{C}$ system at $E(^{14}\text{N})=12.9$ MeV/nucleon yielded results for α -particle correlations and energy spectra consistent with evaporation [15].

In recent years, considerable progress has been made in the development of various theoretical descriptions of preequilibrium emission. Most of these models are based on either the Fermi jet approach [16–18], the Boltzmann master equation [19], or the Landau-Vlasov equation [20]. In general, these models have provided reasonable descriptions of the rather sparse preequilibrium nucleon data that exist. However, these models are appropriate only to explain nucleon emission and it is possible that preequilibrium emission of composite particles is important (for which there are no promising models proposed). A much broader range of nucleon and cluster emission spectra gated on central collisions are needed to provide more severe tests of these models and future efforts in the description of preequilibrium particle emission. It is important to develop a quantitative understanding of preequilibrium particle emission so that it can be used to probe the very early stages of heavy-ion collisions.

In this paper we report on a detailed measurement of protons and α particles emitted in coincidence with evaporation residues for the $^{40}\text{Ca}+^{12}\text{C}$ system at

*Present address: Division of Nuclear Physics, Department of Energy, Washington, D.C. 20585.

$E(^{40}\text{Ca})=450$ MeV. The energy spectra of the evaporation residues and the energy and angular distributions of the light particles are compared with predictions of the statistical model for complete fusion and equilibrium decay. The proton energy spectra are also compared with the predictions of a preequilibrium emission model [18].

The experimental procedure is described in Sec. II. In Sec. III the experimental results are presented. The results are discussed in the context of previous measurements and existing models in Sec. IV, and a summary is presented in Sec. V.

II. EXPERIMENTAL PROCEDURE

The experiment was performed with a pulsed, 450-MeV ^{40}Ca beam from the Argonne National Laboratory ATLAS facility. The time resolution of the beam pulses was better than 200 ps [full width at half maximum (FWHM)] with a period of 82.5 ns. The beam was incident on a $100\text{-}\mu\text{g}/\text{cm}^2$ carbon target mounted in the ATLAS 91-cm scattering chamber. The heavy ions were detected at 4.5° in a large-solid-angle, time-of-flight detector system. This system consists of a parallel-plate avalanche counter for timing and position information and a Bragg-curve spectrometer [21] to obtain the energy and Z identification of the heavy ions. The detector was mounted on the vacuum extension box of the scattering chamber at a distance of 1.00 m from the target and subtended a solid angle of 5.5 msr. The timing information was used to aid in the separation of heavy ions from quasielastic and fusion events. An example of the Z resolution attained is shown in Fig. 1 where the energy is plotted as a function of the range of the heavy ions detected in the Bragg-curve spectrometer.

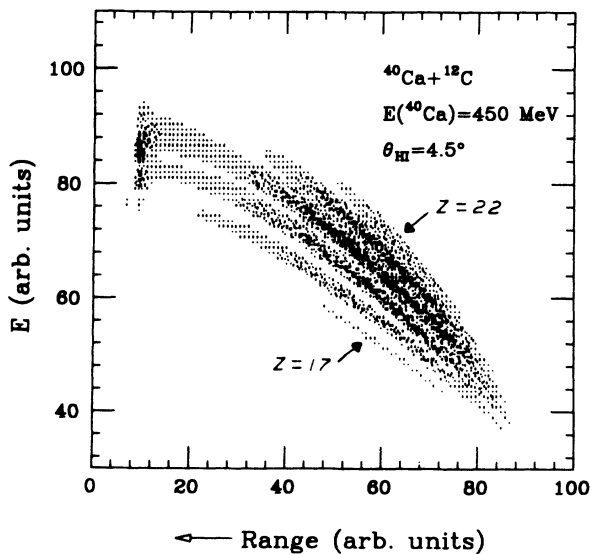


FIG. 1. Two-dimensional spectrum of energy versus range of heavy ions detected in the Bragg-curve spectrometer for $^{40}\text{Ca}+^{12}\text{C}$ at $E(^{40}\text{Ca})=450$ MeV and $\theta_{\text{HI}} = 4.5^\circ$. A gate on the two-dimensional energy versus time-of-flight spectrum was used to exclude quasielastic events from this spectrum.

The light particles were measured at 23 in-plane angles with 12 telescopes consisting of surface-barrier ΔE detectors and lithium-drifted silicon E detectors. The distance of these telescopes from the target ranged from 19.5 to 41.0 cm, and the solid angles varied from 0.577 msr at the most forward angles to 10.75 msr at the backward angles. Identification of the light particles was achieved using the rf-beam timing of ATLAS and is illustrated in Fig. 2. Shown in Fig. 2 is a two-dimensional spectrum of energy deposited in the ΔE detector versus time of flight (TOF) for light particles detected at -55° in coincidence with evaporation residues. The negative angle refers to the opposite side of the beam from the heavy-ion detector.

The energy calibration of the Bragg-curve spectrometer was derived using the alpha groups from a ^{228}Th source and a precision pulser. The slopes of the time-to-amplitude converters (TAC's) used for the TOF measurements of the light particles were determined using a time calibrator. The pedestal (or t_0) for each TAC was obtained using the protons and alpha particles that penetrated the ΔE detectors. The energies of the light particles were then calculated from the TOF calibrations and the measured flight paths.

Signals from the ΔE detectors were used to trigger the electronics. As a result there are high-energy cutoffs in the proton spectra due to the fact that high-energy protons do not lose enough energy in the ΔE detectors to produce signals above the discriminator thresholds. The high-energy cutoff depends on the thickness of the ΔE detector and the discriminator threshold level, but is typically about 30 MeV.

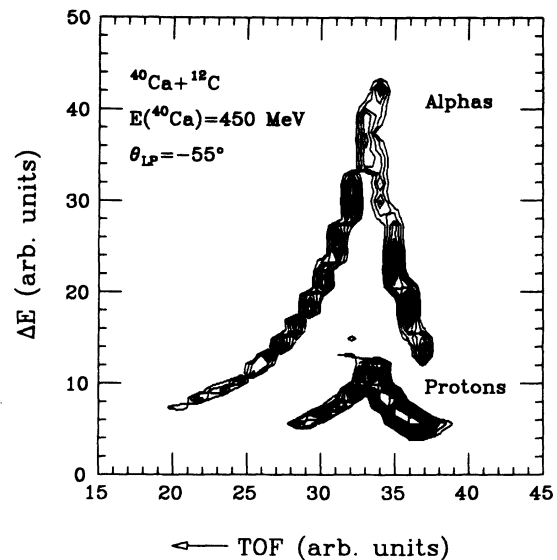


FIG. 2. Two-dimensional spectrum of energy deposited in the ΔE detector versus time of flight (TOF) for light particles detected at -55° in coincidence with evaporation residues detected at 4.5° for $^{40}\text{Ca}+^{12}\text{C}$ at $E(^{40}\text{Ca})=450$ MeV. The negative angle refers to the opposite side of the beam from the heavy-ion detector. The foldover exhibited in the spectrum is due to the fact that the high-energy particles are not stopped in the ΔE detector.

III. EXPERIMENTAL RESULTS

A. Statistical-model calculations

The complete-fusion and equilibrium-decay process has been modeled with the Monte Carlo computer code PACE [22] to aid in the interpretation of the data. This calculation was performed with a total fusion cross section of 900 mb obtained from a surface-friction-model calculation by Frobrich [23] for the $^{16}\text{O}+^{40}\text{Ca}$ system. Discrete energy levels were used for the low-excitation-energy region of each nucleus involved in the evaporation cascades. A level-density parameter of $a = A/8.5 \text{ MeV}^{-1}$ was used at higher excitation energy. An "event" file was created that contained the history of 10^6 cascades. The history includes the mass, charge, and energy of the evaporation residues as well as the energies and angular momenta of the emitted light particles. The file was then scanned with the experimental detector positions and solid angles to construct the energy and angular distributions of the evaporation residues and light particles.

For comparison, the calculation was also performed with the statistical-model code LILITA [24] for fewer cascades. The results of the two calculations were in good agreement.

B. Evaporation residues

Approximately 75% of the evaporation residues detected were isotopes of K, Ca, or Sc. An energy spectrum of Sc residues is shown in Fig. 3. The solid curve is the PACE prediction for complete fusion normalized to the maximum value consistent with the data. The experimental energy distribution is shifted to higher energy than predicted by the PACE calculation, indicating significant incomplete fusion due to preequilibrium emission from the ^{12}C target. This was observed for all

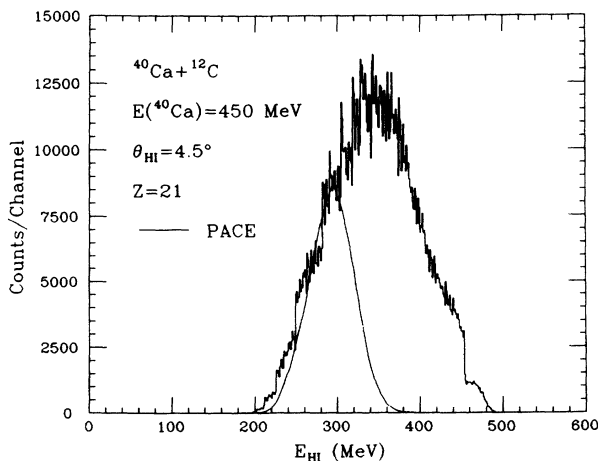


FIG. 3. Energy spectrum of Sc residues detected at 4.5° for $^{40}\text{Ca}+^{12}\text{C}$ at $E(^{40}\text{Ca})=450 \text{ MeV}$. The solid curve is the result of a PACE [22] calculation for the complete-fusion equilibrium-decay process.

residue Z groups. The shape of the spectra was found to be consistent with the assumption that contributions to incomplete fusion corresponding to preequilibrium emission from the ^{40}Ca projectile are negligible. By normalizing the PACE predictions to the maximum value consistent with the data, it is estimated that at most 35% of the evaporation residues arise from complete fusion. These results are consistent with the systematics established by Morgenstern *et al.* [3] from the measurements of inclusive evaporation-residue velocity spectra.

C. α -particle correlations

The energy spectra of α particles measured at $\theta_\alpha = -7^\circ, -27^\circ, -45^\circ, -65^\circ, -95^\circ, +15^\circ, +25^\circ, +45^\circ, +65^\circ,$ and $+75^\circ$ in coincidence with evaporation residues with $12 \leq Z_{\text{ER}} \leq 24$ are shown in Fig. 4. Negative and positive angles refer to the opposite and same side of the beam as the heavy-ion detector, respectively. The vertical scale in the figure indicates the α -particle double-differential multiplicity ($d^2M_\alpha/d\Omega_\alpha dE_\alpha$) defined by

$$\frac{d^2M_\alpha}{d\Omega_\alpha dE_\alpha} = \frac{d^3\sigma/d\Omega_\alpha d\Omega_{\text{HI}} dE_\alpha}{(d\sigma/d\Omega_{\text{HI}})_{\theta_{\text{HI}}}},$$

where $(d\sigma/d\Omega_{\text{HI}})_{\theta_{\text{HI}}}$ is the differential cross section of the evaporation residues measured at $\theta_{\text{HI}} = 4.5^\circ$. The solid curves shown in the figure are the results of the PACE calculation for complete fusion and equilibrium decay. The agreement with the data at forward angles ($|\theta_\alpha| \leq 45^\circ$) is quite reasonable except at the most forward angles on the opposite side of the beam. The experimental spectrum at -7° shows a large probability of α particles with energies between 25 and 65 MeV which is not predicted by the calculation. Also, the high-energy slope of the experimental spectra at -7° and -27° are steeper than

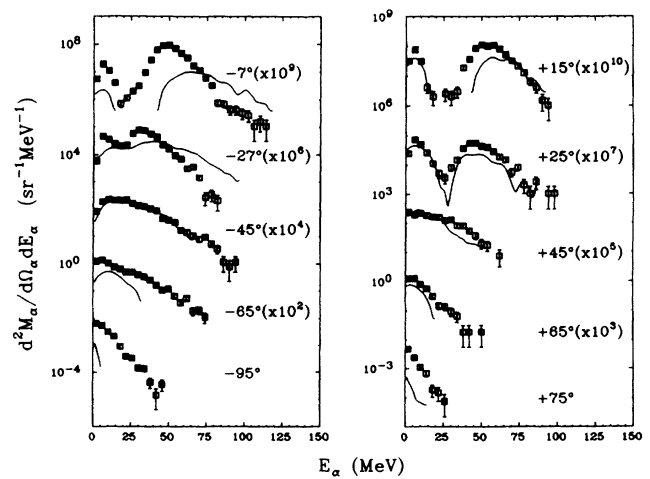


FIG. 4. Energy spectra of α particles detected in coincidence with evaporation residues ($12 \leq Z_{\text{ER}} \leq 24$) observed at 4.5° . Negative and positive angles refer to the opposite and same side of the beam as the heavy-ion detector, respectively. The solid curves are the results of PACE [22] calculations for the complete-fusion equilibrium-decay process.

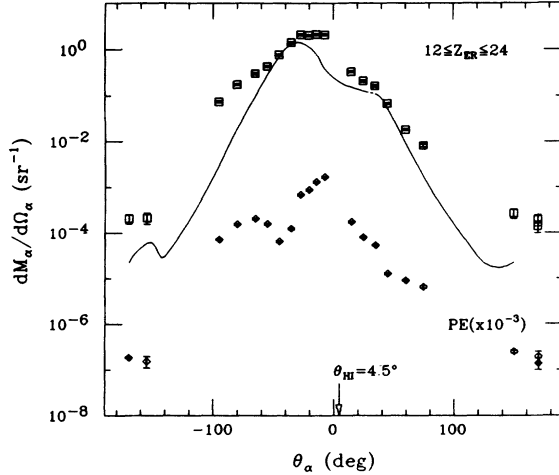


FIG. 5. Angular correlation of α particles with evaporation residues ($12 \leq Z_{ER} \leq 24$) detected at 4.5° (squares). The solid curve is the result of the complete-fusion equilibrium-decay calculation performed with the code PACE [22]. The diamonds indicate the angular distribution of preequilibrium (PE) α particles obtained by subtracting the calculation from the data.

predicted. At angles larger than 45° the calculations underpredict the experimental spectra.

Integrating over the α -particle energy spectra, we obtain the angular correlation (squares) shown in Fig. 5. The solid curve is the statistical-model prediction for complete fusion and equilibrium decay. The calculation provides a good description of the data at angles around 45° on both sides of the beam; however, it underpredicts the data at the more forward and backward angles.

The angular correlations of α particles with residues of K, Ca, and Sc are shown in Fig. 6. The solid curves shown in the figure are the results of the statistical-model calculation for complete fusion and equilibrium decay.

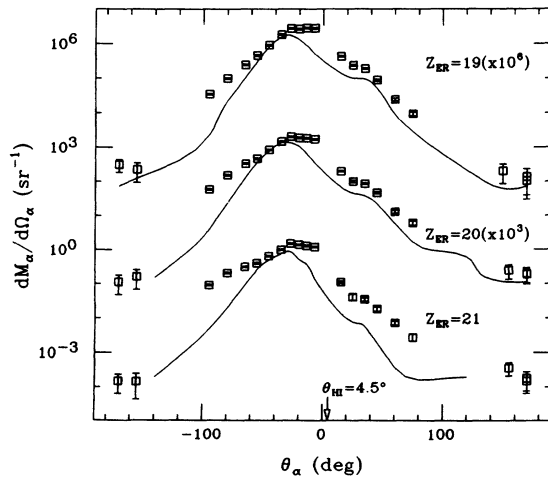


FIG. 6. Angular correlations of α particles with residues of K, Ca, and Sc detected at 4.5° . The solid curves are the results of PACE [22] calculations for the complete-fusion equilibrium-decay process.

From this figure it can be seen that the discrepancies between the data and the calculation become more pronounced with increasing Z of the evaporation residues.

D. Proton correlations

Although the experiments were primarily designed for α -particle correlations with heavy ions, protons were also detected in these measurements. The energy spectra of protons measured at $\theta_P = -7^\circ, -45^\circ, -95^\circ, -140^\circ, -170^\circ, +25^\circ, +45^\circ, +75^\circ, +120^\circ,$ and $+150^\circ$ in coincidence with evaporation residues with $12 \leq Z_{ER} \leq 24$ are shown in Fig. 7. The solid curves are the results of the PACE calculation for complete fusion and equilibrium decay. The agreement between the data and the predictions at forward angles is poor. The experimental spectra at -7° and $+25^\circ$ show an enhanced yield at low energies. Also, the high-energy slopes of the forward-angle spectra are steeper than predicted. The agreement between the data and the calculations improves at larger angles and is fairly good at -95° and $+75^\circ$ as shown in the figure. However, at backward angles the statistical model underpredicts the experimental spectra.

The angular correlation obtained by integrating the proton energy spectra (squares) is compared with the PACE prediction for complete fusion and equilibrium decay (solid curve) in Fig. 8. The calculation overpredicts most of the data at forward angles and underpredicts the data at backward angles. The overprediction of the data at forward angles may, at least in part, be due to the high-energy cutoffs in the proton energy spectra.

The angular correlations of protons with residues of K, Ca, and Sc are shown in Fig. 9. The solid curves shown in the figure are the results of the statistical-model calculation for complete fusion and equilibrium decay. As in

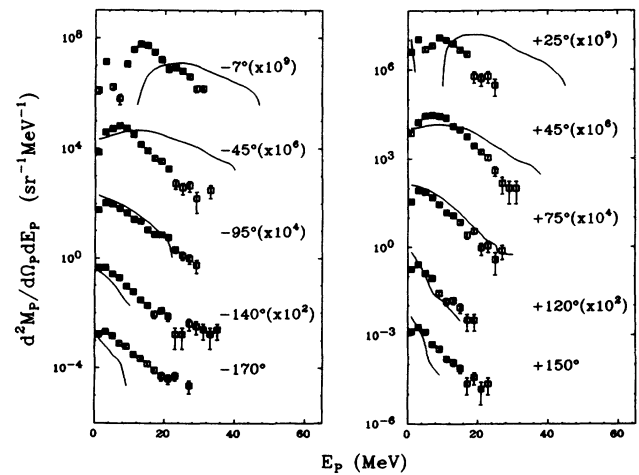


FIG. 7. Energy spectra of protons detected in coincidence with evaporation residues ($12 \leq Z_{ER} \leq 24$) observed at 4.5° . Negative and positive angles refer to the opposite and same side of the beam as the heavy-ion detector, respectively. The solid curves are the results of PACE [22] calculations for the complete-fusion equilibrium-decay process.

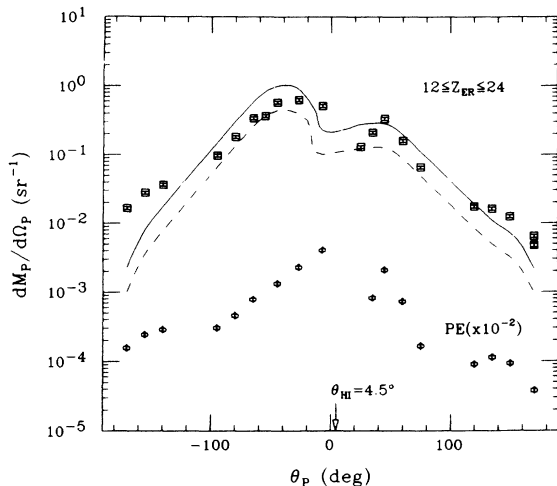


FIG. 8. Angular correlation of protons with evaporation residues ($12 \leq Z_{ER} \leq 24$) detected at 4.5° (squares). The solid curve is the result of the complete-fusion equilibrium-decay calculation performed with the code PACE [22]. The dashed curve is the calculation normalized to the data at $\theta_P = -55^\circ$. The diamonds indicate the angular distribution of preequilibrium (PE) protons obtained by subtracting the renormalized calculation from the data.

the case of the α correlations, the discrepancies between the data and the calculation become more pronounced with increasing Z of the evaporation residues.

IV. DISCUSSION

There is clear and consistent evidence from the data of preequilibrium emission of both α particles and protons from the target. The evaporation-residue energy spectra (Fig. 3) are shifted to higher energy than predicted by PACE and expected from the reaction kinematics for

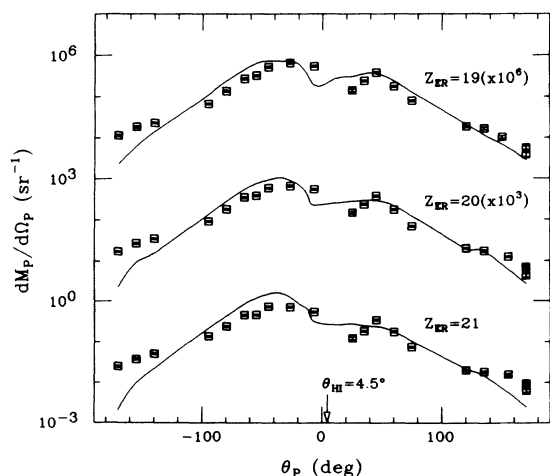


FIG. 9. Angular correlations of protons with residues of K, Ca, and Sc detected at 4.5° . The solid curves are the results of PACE [22] calculations for the complete-fusion equilibrium-decay process.

complete fusion. This indicates that there is significant incomplete fusion due to preequilibrium emission from the target. Also, the α -particle and proton yields at backward angles are much larger than predicted by the statistical model. One would expect that any preequilibrium particles emitted from the target will be detected at large angles. In fact, due to the reverse kinematics employed in this reaction, nearly all of the statistical light particles fall in the forward hemisphere and, therefore, the light particles detected at backward angles in coincidence with evaporation residues are almost exclusively preequilibrium. It should also be pointed out that light particles evaporated from a reduced compound nucleus formed in an incomplete-fusion reaction due to preequilibrium emission from the target will be even more forward focused since the reduced compound nucleus will be moving with a higher velocity than the complete-fusion compound nucleus.

From the comparisons of the PACE predictions for complete fusion with the data, there is conflicting evidence both for and against significant preequilibrium emission from the projectile. The shapes of the energy spectra of the evaporation residues are consistent with the assumption that preequilibrium emission from the projectile is negligible. These observations are compatible with the results of earlier inclusive measurements [1–10] of evaporation-residue velocity distributions which indicate that emission from the lighter reaction partner is dominant. The estimate that an upper limit of 35% of the evaporation residues arises from complete fusion is also in agreement with the systematics established by Morgestern *et al.* [3] and supported by recent measurements [6–9]. This estimate was obtained by normalizing the PACE predictions for complete fusion to the maximum value consistent with the data with the assumption that preequilibrium emission from the projectile is negligible.

On the other hand, comparisons of the statistical-model predictions for complete fusion and equilibrium decay with the light-particle data suggest that there may be preequilibrium emission from the projectile. There appears to be beam-velocity components in the energy spectra at forward angles for both α particles (Fig. 4) and protons (Fig. 7). An α particle traveling with the beam velocity would have an energy of 45 MeV, while a beam-velocity proton would have an energy of 11 MeV. Light particles traveling at the beam velocity are expected in the simplest pictures of incomplete fusion due to preequilibrium emission from the projectile. Also, from a comparison of the experimental (squares) and calculated (solid curve) α -particle angular correlations shown in Fig. 5, it can be seen that the calculation underpredicts the data at forward angles as well as at backward angles. After subtracting the calculation from the data, we obtain the angular distribution of the apparent nonstatistical component shown as the diamonds in Fig. 5. This distribution is forward peaked and roughly symmetric around the beam which is also expected in the simplest pictures of incomplete fusion due to preequilibrium emission from the projectile. There is also a second peak in the distribution centered around -70° which might be taken as evidence that some α particles escape from the

projectile with a substantial transverse velocity component and not simply in the initial beam direction. Evidence for this type of process has been reported [25] for $^{12}\text{Ca}+^{197}\text{Au}$, ^{160}Gd , and ^{120}Sn reactions at $E(^{12}\text{C})=5.5\text{--}10$ MeV/nucleon where it was found that the angular distributions for incomplete fusion peaked at significantly larger angles than those for complete fusion.

The proton differential multiplicities (squares) shown in Fig. 8 are overpredicted by the PACE calculation for complete fusion and equilibrium decay (solid curve) at most of the forward angles. As mentioned earlier, this may, at least in part, be due to the high-energy cutoffs in the proton energy spectra. If we assume that the shape of the calculation is correct and normalize it to the data at -55° , we obtain the dashed curve shown in the figure. Comparing the shape of the normalized calculation with the experimental distribution, an extra component is apparent. The angular distribution of this extra component was obtained by subtracting the renormalized calculation from the data and is shown as the diamonds in Fig. 8. As with the α correlations, this distribution is roughly symmetric around the beam direction and peaked at forward angles.

Another discrepancy between the data and the PACE calculation for complete fusion is that the high-energy slopes of the proton spectra measured at forward angles are steeper than the predictions. A similar, although less dramatic, disagreement is seen for the α -particle spectra measured at forward angles on the opposite side of the beam from the heavy-ion detector. Statistical-model calculations for the formation of reduced compound nuclei that might be formed in a simple picture of incomplete fusion suggest that this is not a simple effect due to the presence of incomplete fusion.

Since nearly all of the light particles observed at backward angles ($\theta > 65^\circ$ for α particles and $\theta > 120^\circ$ for

protons) in coincidence with evaporation residues are of preequilibrium origin, the large-angle spectra should provide a good test for preequilibrium emission models. Shown in Fig. 10 are averaged proton energy spectra compared with the predictions of the nucleon-exchange-transport model for preequilibrium emission [18] (solid curves). The experimental distributions were obtained by averaging energy spectra taken at the same angle on either side of the beam to remove the experimental asymmetry and facilitate the comparison with the preequilibrium-emission model. The model overpredicts the high-energy portion of the energy spectra at forward angles. As one goes back in angle, the agreement between the calculation and the data improves, and at 75° it is quite good. However, at backward angles the calculation overpredicts the spectra. Emission at backward angles is induced in the model by nucleons originating in the target and propagating through the projectile. Similar discrepancies between the predictions and data at backward angles have been observed previously [18].

V. SUMMARY

We have performed a detailed measurement of α particles and protons emitted in coincidence with evaporation residues produced in the $^{40}\text{Ca}+^{12}\text{C}$ reaction using a pulsed 450-MeV ^{40}Ca beam from the ATLAS facility. The evaporation residues were detected and Z identified with a large-solid-angle, time-of-flight detector system. Energy spectra were obtained for each evaporation-residue Z group. These energy spectra are shifted to higher energy than expected for complete fusion, indicating the presence of significant incomplete fusion due to preequilibrium emission from the ^{12}C target. The shape of the evaporation-residue energy spectra is consistent with the assumption that incomplete fusion due to emission from the projectile is negligible. Comparisons of the evaporation-residue energy spectra with statistical-model predictions for complete fusion suggest that at most 35% of the evaporation residues arise from complete fusion.

Energy and angular distributions were generated for α particles and protons in coincidence with each evaporation-residue Z group. The light-particle yield at backward angles are much larger than predicted by the statistical model and expected from reaction kinematics for complete fusion and equilibrium decay, indicating the presence of considerable preequilibrium emission of both α particles and protons from the ^{12}Ca target. Comparisons of the forward-angle, light-particle data with statistical-model predictions for complete fusion also suggest that there may be preequilibrium emission from the projectile in contradiction with the results from the evaporation-residue energy spectra.

We have also compared the averaged proton energy spectra with the predictions of the nucleon-exchange-transport model for preequilibrium emission [18]. While the agreement between the calculation and the data is reasonable at 75° , the calculated proton spectra are harder than the data at forward angles and overpredict the yields at backward angles.

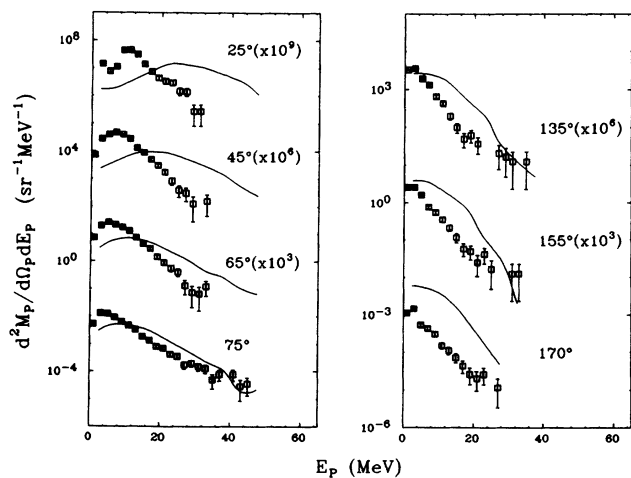


FIG. 10. Averaged energy spectra of protons detected in coincidence with evaporation residues ($12 \leq Z_{\text{ER}} \leq 24$) observed at 4.5° . The spectra were obtained by averaging the energy spectra taken at the same angle on either side of the beam. The solid curves are the results of calculations with the nucleon-exchange transport model for preequilibrium emission [18].

ACKNOWLEDGMENTS

We would like to thank Prof. R. Vandenbosch for performing calculations with the nucleon-exchange-transport model. This work was supported by the U.S. Department of Energy under Contracts Nos. DE-FG05-88ER40459 and W-31-109-ENG-38.

-
- [1] H. Morgenstern, W. Bohne, K. Grabisch, D. G. Kovar, and H. Lehr, *Phys. Lett.* **113B**, 463 (1982); H. Morgenstern, W. Bohne, K. Grabisch, H. Lehr, and W. Stoffler, *Z. Phys. A* **313**, 39 (1983).
- [2] Y. Chan, M. Murphy, R. G. Stokstad, I. Tserruya, S. Wald, and A. Budzanowski, *Phys. Rev. C* **27**, 447 (1983).
- [3] H. Morgenstern, W. Bohne, W. Galster, K. Grabisch, and A. Kyanowski, *Phys. Rev. Lett.* **52**, 1104 (1984).
- [4] G. Rosner, J. Pochodzalla, B. Heck, G. Hlawatsch, A. Miczaika, J. H. Rabe, R. Butsch, B. Kolb, and B. Sedelmeyer, *Phys. Lett.* **150B**, 87 (1985).
- [5] G. S. F. Stephans, D. G. Kovar, R. V. F. Janssens, G. Rosner, H. Ikezoe, B. Wilkins, D. Henderson, K. T. Lesko, J. J. Kolata, C. K. Gelbke, B. V. Jacack, Z. M. Koenig, G. D. Westfall, A. Szanto De Toledo, E. M. Szanto, and P. L. Gonthier, *Phys. Lett.* **161B**, 60 (1985).
- [6] C. Beck, D. G. Kovar, S. J. Sanders, B. D. Wilkins, D. J. Henderson, R. V. F. Janssens, W. C. Ma, M. F. Vineyard, T. F. Wang, C. F. Maguire, F. W. Prosser, and G. Rosner, *Phys. Rev. C* **39**, 2202 (1989).
- [7] M. F. Vineyard, J. S. Bauer, C. H. Gosdin, R. S. Trotter, D. G. Kovar, C. Beck, D. J. Henderson, R. V. F. Janssens, B. D. Wilkins, G. Rosner, P. Chowdhury, H. Ikezoe, W. Kuhn, J. J. Kolata, J. D. Hinnefeld, C. F. Maguire, J. F. Mateja, F. W. Prosser, and G. S. F. Stephans, *Phys. Rev. C* **41**, 1005 (1990).
- [8] M. F. Vineyard, J. S. Bauer, J. F. Crum, C. H. Gosdin, R. S. Trotter, D. G. Kovar, C. Beck, D. J. Henderson, R. V. F. Janssens, B. D. Wilkins, C. F. Maguire, J. F. Mateja, F. W. Prosser, and G. S. F. Stephans, *Phys. Rev. C* **45**, 1784 (1992).
- [9] M. F. Vineyard, J. F. Mateja, C. Beck, S. E. Atencio, L. C. Dennis, A. D. Frawley, D. J. Henderson, R. V. F. Janssens, K. W. Kemper, D. G. Kovar, C. F. Maguire, S. J. Padalino, F. W. Prosser, G. S. F. Stephans, M. A. Tiede, B. D. Wilkins, and R. A. Zingarelli, *Phys. Rev. C* **47**, 2374 (1993).
- [10] G. P. Gilfoyle, M. S. Gordon, R. L. McGrath, G. Auger, J. M. Alexander, D. G. Kovar, M. F. Vineyard, C. Beck, D. J. Henderson, P. A. DeYoung, and D. Kortering, *Phys. Rev. C* **46**, 265 (1992).
- [11] H. Morgenstern, W. Bohne, W. Galster, and K. Grabisch, *Z. Phys. A* **324**, 443 (1986).
- [12] H. Ikezoe, N. Shikazono, Y. Tomita, Y. Sugiyama, and K. Ideno, *Nucl. Phys.* **A462**, 150 (1987).
- [13] P. Gonthier, H. Ho, M. N. Namboodiri, L. Adler, J. B. Natowitz, S. Simon, K. Hagel, R. Terry, and A. Khodai, *Phys. Rev. Lett.* **44**, 1387 (1980); P. L. Gonthier, H. Ho, M. N. Namboodiri, J. B. Natowitz, L. Adler, S. Simon, K. Hagel, S. Kniffen, and A. Khodai, *Nucl. Phys.* **A411**, 289 (1983).
- [14] K. A. Griffioen, E. A. Bakkum, P. Decowski, R. J. Meijer, and R. Kamermans, *Phys. Rev. C* **37**, 2502 (1988).
- [15] J. Gomez del Campo, D. E. DiGregorio, J. A. Biggerstaff, Y. D. Chan, D. C. Hensley, P. H. Stelson, D. Shapira, and M. E. Ortiz, *Phys. Rev. C* **35**, 137 (1987).
- [16] S. Leray, G. La Rana, C. Ngo, M. Barranco, M. Pi, and X. Vinas, *Z. Phys. A* **320**, 383 (1985).
- [17] K. Mohring, W. J. Swiatecki, and M. Zielinska-Pfabe, *Nucl. Phys.* **A440**, 89 (1985).
- [18] J. Randrup and R. Vandenbosch, *Nucl. Phys.* **A474**, 2129 (1987); S. J. Luke, R. Vandenbosch, and J. Randrup, *Phys. Rev. C* **48**, 857 (1993).
- [19] M. Blann, *Phys. Rev. C* **31**, 295 (1985); **32**, 1231 (1985).
- [20] C. Gregoire, B. Remaud, F. Scheuter, and F. Sebillie, *Nucl. Phys.* **A436**, 365 (1985).
- [21] M. F. Vineyard, B. D. Wilkins, D. J. Henderson, D. G. Kovar, C. Beck, C. N. Davids, and J. J. Kolata, *Nucl. Instrum. Methods A* **255**, 507 (1987).
- [22] PACE is the modification of the code JULIAN described by A. Gavron, *Phys. Rev. C* **21**, 230 (1980).
- [23] P. Frobrich, *Phys. Rep.* **116**, 337 (1984).
- [24] J. Gomez del Campo and R. G. Stokstad, Oak Ridge National Laboratory Technical Report No. ORNL-TM-7295, 1981 (unpublished).
- [25] I. Tserruya, V. Steiner, Z. Fraenkel, P. Jacobs, D. G. Kovar, W. Henning, M. F. Vineyard, and B. G. Glagola, *Phys. Rev. Lett.* **60**, 14 (1988).